



The impact of isolated lesions on white-matter fiber tracts in multiple sclerosis patients



Amgad Droby^{a,b}, Vinzenz Fleischer^{a,b}, Marco Carnini^c, Hilga Zimmermann^{a,b}, Volker Siffrin^a, Joachim Gawehn^d, Michael Erb^e, Andreas Hildebrandt^c, Bernhard Baier^{a,b,1}, Frauke Zipp^{a,b,*,1}

^aDepartment of Neurology, University Medical Center of the Johannes Gutenberg University, Mainz, Germany

^bNeuroimage Center (NIC) of the Focus Program Translational Neuroscience (FTN), Johannes Gutenberg University, Mainz, Germany

^cDepartment of Computer Science, Johannes Gutenberg University, Mainz, Germany

^dDepartment of Neuroradiology, University Medical Center of the Johannes Gutenberg University, Mainz, Germany

^eDepartment of Biomedical Magnetic Resonance, University Hospital, Tübingen, Germany

ARTICLE INFO

Article history:

Received 27 January 2015

Accepted 8 March 2015

Available online 10 April 2015

Keywords:

Multiple sclerosis
Diffusion tensor imaging
Fractional anisotropy
Brainstem
White matter

ABSTRACT

Infratentorial lesions have been assigned an equivalent weighting to supratentorial plaques in the new McDonald criteria for diagnosing multiple sclerosis. Moreover, their presence has been shown to have prognostic value for disability. However, their spatial distribution and impact on network damage is not well understood. As a preliminary step in this study, we mapped the overall infratentorial lesion pattern in relapsing–remitting multiple sclerosis patients ($N = 317$) using MRI, finding the pons (lesion density, $14.25/\text{cm}^3$) and peduncles ($13.38/\text{cm}^3$) to be predilection sites for infratentorial lesions. Based on these results, 118 fiber bundles from 15 healthy controls and a subgroup of 23 patients showing lesions unilaterally at the predilection sites were compared using diffusion tensor imaging to analyze the impact of an isolated infratentorial lesion on the affected fiber tracts. Fractional anisotropy, mean diffusion as well as axial and radial diffusivity were investigated at the lesion site and along the entire fiber tract. Infratentorial lesions were found to have an impact on the fractional anisotropy and radial diffusivity not only at the lesion site itself but also along the entire affected fiber tract. As previously found in animal experiments, inflammatory attack in the posterior fossa in multiple sclerosis impacts the whole affected fiber tract. Here, this damaging effect, reflected by changes in diffusivity measures, was detected in vivo in multiple sclerosis patients in early stages of the disease, thus demonstrating the influence of a focal immune attack on more distant networks, and emphasizing the pathophysiological role of Wallerian degeneration in multiple sclerosis.

© 2015 The Authors. Published by Elsevier Inc. This is an open access article under the CC BY-NC-ND license (<http://creativecommons.org/licenses/by-nc-nd/4.0/>).

1. Introduction

In the revised McDonald criteria, the dissemination of lesions in infratentorial regions has been assigned an equal weighting to those in the supratentorial region and spinal cord, emphasizing their significance in the diagnosis of multiple sclerosis (MS) (Polman et al., 2011). Such lesions are thought to be specific to MS (Miller et al., 1987) and their detection using magnetic resonance imaging (MRI) has been

found to be a predictor for long-term disability (Minneboo et al., 2004), and indeed, the presence of at least one brainstem lesion has been found to represent an increased risk of disability (Tintore et al., 2010). These studies investigating infratentorial lesions in MS have focused on their prevalence and effects on clinical outcome (Minneboo et al., 2004; Tintore et al., 2010); however, the pathophysiological effects of infratentorial lesions on white matter (WM) tracts in MS remain unclear. Using the experimental autoimmune encephalomyelitis (EAE) model, it has been demonstrated that MS lesions lead to axonal dissection and damage in sites distant to the autoimmune attack itself (Siffrin et al., 2010a). Local damage resulting from MS lesions has been reported in MS patients (Ciccarelli et al., 2008; Filippi et al., 2001; Rovaris et al., 2005), but their impact along WM fibers prior to complete transection is not well understood.

White-matter tissue can be specifically visualized using diffusion tensor imaging (DTI) (Beaulieu, 2002) and brain pathways can then be traced in vivo via fiber tractography (Ciccarelli et al., 2008; Mori and van Zijl, 2002). In DTI, MS lesions typically manifest as a local

Abbreviations: AD, axial diffusivity; EAE, experimental autoimmune encephalomyelitis; FA, fractional anisotropy; ICP, inferior cerebellar peduncle; LD, lesion density; LSAF, left superior arcuate fasciculus; MD, mean diffusivity; NAWM, normal-appearing white matter; RD, radial diffusivity.

* Corresponding author at: Department of Neurology, University Medical Center of the Johannes Gutenberg University Mainz, Neuroimage Center (NIC) of the Focus Program Translational Neuroscience (FTN), Langenbeckstr. 1, 55131 Mainz, Germany. Tel.: +49 (0)6131 17 7156; fax: +49 (0)6131 17 5697.

E-mail address: frauke.zipp@unimedizin-mainz.de (F. Zipp).

¹ Both authors contributed equally.

reduction in fractional anisotropy (FA) and increase in mean diffusivity (MD) within the lesioned area (Ciccarelli et al., 2008; Filippi et al., 2001). By exploiting directional diffusivities, it has been demonstrated in mouse models of WM pathology that decreased axial diffusivity (AD) can be associated with axonal injury and increased radial diffusivity (RD) with demyelination (Song et al., 2003; Song et al., 2005). Furthermore, patients with relapsing–remitting MS (RRMS) (Pagani et al., 2005) and clinically isolated syndrome (CIS) (Lin et al., 2007) were shown to have abnormal diffusion indices in the corticospinal tract that correlated with lesion load, which was interpreted as being associated with ongoing pathologic processes such as Wallerian degeneration and diffuse inflammation (Ciccarelli et al., 2008). Previous *in vivo* studies using DTI and tractography in MS patients have demonstrated changes in DTI measures along fibers affected by MS lesions; however, these changes were not associated with the effects of an isolated lesion (Bammer et al., 2000; Rocca et al., 2013; Walsh et al., 2011). In a combined post-mortem histology and MRI study, Kolasinski et al. were able to demonstrate diffuse WM damage as a result of a focal MS lesion reflected by DTI measures. This was found to correlate with histological measures of myelin integrity (Kolasinski et al., 2012).

In this work, we aimed to investigate the impact of MS lesions *in vivo* on WM fibers in RRMS patients using DTI measures. Due to a lack of reports regarding the predilection sites of lesions in the brain stem, a preliminary lesion mapping study was performed on a large patient cohort in order to identify regions of interest for the subsequent DTI analysis. Then, the main focus of this work was to investigate the impact that an isolated lesion has on diffusivity measures in affected WM fiber tracts by comparison to corresponding contralateral non-lesioned fibers in those patients and to healthy controls. We could show that diffusivity measures are not only affected locally at the lesion site but along the entire fiber tract.

2. Method

This study was approved by the local ethical committee and was conducted in accordance with the declaration of Helsinki. All participants gave their informed consent for participating in this study.

2.1. Subjects

In total 317 patients with RRMS were examined using MRI (215 using a 1.5-T scanner and 102 with a 3-T scanner). All patients were diagnosed according to the revised McDonald criteria (Polman et al., 2011). In the 1.5- and 3-T cohorts, 106 (49%) and 68 (67%) patients, respectively, showed infratentorial lesions in T2-weighted MRI. The mean age of these patients was 35 y (SD = ± 10 y), with a mean disease duration of 6.1 y (± 5.8 y) and median expanded disability status scale (EDSS) score of 1.5 (range 0–6.5).

2.2. Magnetic resonance acquisition

For the lesion mapping study (see details below), data were collected on either a 1.5 or 3-T scanner. Data for the fiber tractography analysis was collected on the 3-T scanner only. T2-weighted images were obtained using a 1.5-T whole-body MR scanner with the standard head coil. The measurement parameters for the turbo spin echo (TSE) sequence were: TR = 3000 ms, TE = 175 ms, 160 sagittal slices with slice thickness 1 mm, and FOV = 256 × 208 mm². Data were also recorded using a 3-T MR scanner (Magnetom TimTrio®, Siemens, Germany) with a 32-channel head coil and using the following protocol: 3D T1-weighted MP-RAGE sequence (TI = 900 ms, TR = 1900 ms, TE = 2.52 ms, FOV = 256 × 265 mm², flip angle = 9°, voxel size = 1 × 1 × 1 mm³, 192 slices). 3D T2-weighted TSE sequence (TR = 500 ms, TE = 79 ms, FOV = 256 × 256 mm², flip angle = 120°, voxel size = 1 × 1 × 1 mm³, 192 slices); and 2D T2-FLAIR sequence (TR = 9000 ms, TE = 79 ms, FOV = 210 × 210 mm², flip angle = 150°,

voxel size = 1 × 1 mm², 45 slices, slice thickness = 3 mm, slice gap = 2 mm). The diffusion data were obtained using a single-shot DW EPI sequence (TR = 9000 ms, TE = 102 ms, 30 directions, *b* = 0 and 900 s/mm², FOV = 256 × 256 mm², matrix size = 128 × 128, flip angle = 90°, 62 slices slice thickness = 2 mm and gap = 0.5 mm, voxel size = 2 × 2 mm², number of averages = 1).

2.3. Lesion mapping

The preliminary lesion mapping study, conducted retrospectively to select regions of interest in the brain stem to be used in the subsequent DTI analysis, included all 317 patients. To define regional vulnerability to MS lesions, a lesion density (LD) map was calculated by relating the probability of plaques to the volume of the corresponding region using the MRICroN software (Baier et al., 2012; Rorden et al., 2007) (<https://www.nitrc.org/projects/mricron>). To create the lesion overlay map, T2-weighted WM lesion boundaries were firstly delineated on the T1-weighted images and then transposed onto a T1 Montreal Neurological Institute (MNI) template by an experienced operator (VF). The extension and location of the lesion shapes was controlled by a second experienced operator (AD).

2.4. Post-processing of diffusion data and tractography

Building on the preliminary lesion-mapping study, DTI data were selected from the 3-T cohort only for tractography analysis based on lesions being found unilaterally at the inferior cerebellar peduncle (ICP; *N* = 21), or for comparison, at the left superior arcuate fasciculus (LSAF) fiber tracts (*N* = 23), which are commonly affected by MS lesions (Rossi et al., 2012). Fifteen age-matched healthy controls (HC) were also sampled on the same MR system. The ICP was located using a DTI atlas (Wakana et al., 2004). All DTI data were post-processed using the SPM8 diffusion toolbox (<http://www.sourceforge.net/projects/spmtools/>). Images were co-registered and re-sliced to the b0 image for motion correction. FA and MD maps were calculated. For the tractography, the lesion mask was used to define the seed points, which were determined individually in native space. Contralateral fibers were also extracted and considered as normal-appearing white matter (NAWM) fibers. The affected fibers were screened by an experienced operator to ensure the presence of only one single lesion along the fibers, and in the case of NAWM fibers that no lesion was present. Seed points were marked in HCs in order to extract corresponding fibers.

Tensor estimation and fiber tracking was performed using the MedINRIA DTI Track software (<http://www.sop.inria.fr/asclepios/software/MedINRIA/>) employing the streamline approach for tractography using angle and anisotropy thresholds of 0.2 and 0.3, respectively. Additional steps such as controlling the volume, length, and angulation, as well as employing Hausdorff mean gravity in order to remove outliers of the retraced fibers were taken to minimize possible inherent artifacts, particularly in brainstem regions.

2.5. Fiber tract-oriented statistics

After extracting target fibers from MedINRIA, they were normalized and bundled by volume and length using the built-in length, center of mass-based fiber gravity, and Hausdorff distance-based fiber-set clustering algorithms in the Fiberviewer© software (Corouge et al., 2006). The DTI indices were plotted along the entire tract arc length as a function of the geodesic distance from the lesion site center in patients or the corresponding site in NAWM and HC groups. The distribution function of each diffusion component was compared using the Kolmogorov–Smirnov test.

3. Results

3.1. Lesion mapping

Lesion accumulation in the affected infratentorial areas in RRMS patients is shown in Fig. 1. The highest LD was found in the brainstem and cerebellar peduncles, particularly ventral and ventrolateral to the fourth ventricle in the boundary between the pons and peduncles (Fig. 1B). The cerebellar hemispheres showed disseminated lesions with barely overlapping lesions. Of the total 728 lesions, 380 (52%), 295 (41%), 20 (3%) and 19 (3%) were observed in the cerebellar peduncles, pons, mesencephalon and medulla oblongata, respectively, for which LD values of $13.38/\text{cm}^3$, 14.25 , $2.44/\text{cm}^3$, and $2.84/\text{cm}^3$ were calculated, respectively.

3.2. DTI and fiber tracking of the ICP

One of the most common infratentorial predilection sites was found to be within the cerebellar peduncles, with 21 of the 3-T patients found to have a lesion affecting the right ICP fiber tract. The tracts of these 21 patients were compared with contralateral NAWM-ICP tracts and corresponding tracts in HCs; in total, 57 ICP fibers were investigated.

Directly at the lesion site, FA values decreased in the ipsilesional fibers in the 21 patients with lesions affecting the ICP compared to the corresponding site in HC and contralateral NAWM ($p < 0.001$). Moreover, a decrease in FA was also observed in the contralateral NAWM relative to HC ($p < 0.05$). RD was found to be increased at the lesion site in patients compared with corresponding sites in HC ($p < 0.001$) and NAWM ($p = 0.05$) (Fig. 2). No differences were detected with respect to MD or AD (MD, $p = 0.43$; AD, $p = 0.72$).

Fig. 3A–E show that the DTI indices along the entire ICP fibers passing through MS lesions (Fig. 3A). FA values along ICP fibers were found to be lower in ipsilesional WM fibers compared to HC ($p < 0.05$) (see Fig. 3B). RD showed an increase along the tracked ipsilesional fibers compared to the HC group ($p < 0.05$) (see Fig. 3E). No differences in MD and AD values were observed between the three groups ($p = 0.39$).

3.3. DTI and fiber tracking of the LSAF

Diffusivity parameters were compared for 23 patients whose LSAF fibers were affected by one periventricular lesion. To ensure a valid

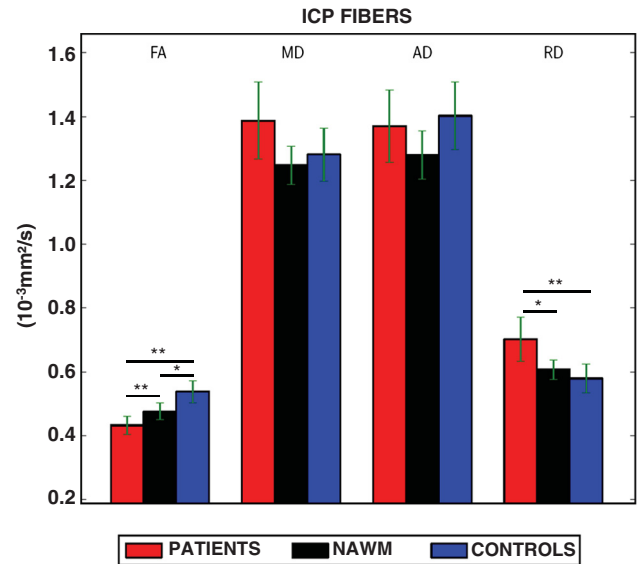


Fig. 2. Diffusion indices at the lesion site of the ICP bar chart of diffusion indices at the lesion site of the inferior cerebellar peduncle (ICP). Error bars indicate standard deviation from the mean (SD). Fractional anisotropy (FA), mean diffusion (MD), axial diffusivity (AD) and radial diffusivity (RD) at the lesion site in ICP fibers or at the corresponding contralateral NAWM site in the same patients and healthy controls (HC). Reduced FA values are found at the lesion site and NAWM site compared to the same site in HC. RD was increased at the lesion site in comparison with the corresponding contralateral site in NAWM and HC fibers. There are no differences between the three groups with respect to MD and AD ($*p < 0.05$; $**p < 0.01$; Kolmogorov–Smirnov test).

comparison and avoid confounding variables, the analysis was performed in the same way for the ICP fibers. Again, contralateral NAWM fibers in the same patients and corresponding fibers in HCs were analyzed for comparison. In total, 61 LSAF fibers were investigated. Fig. 4A–F show the DTI indices along the entire LSAF fibers passing through an MS lesion. A comparison of FA along the entire fibers indicated a reduction in the ipsilesional fibers compared to HC and contralateral NAWM ($p < 0.01$) (Fig. 4B), whereas MD, AD and RD were found to be increased ($p < 0.01$) (see Fig. 4C–E).

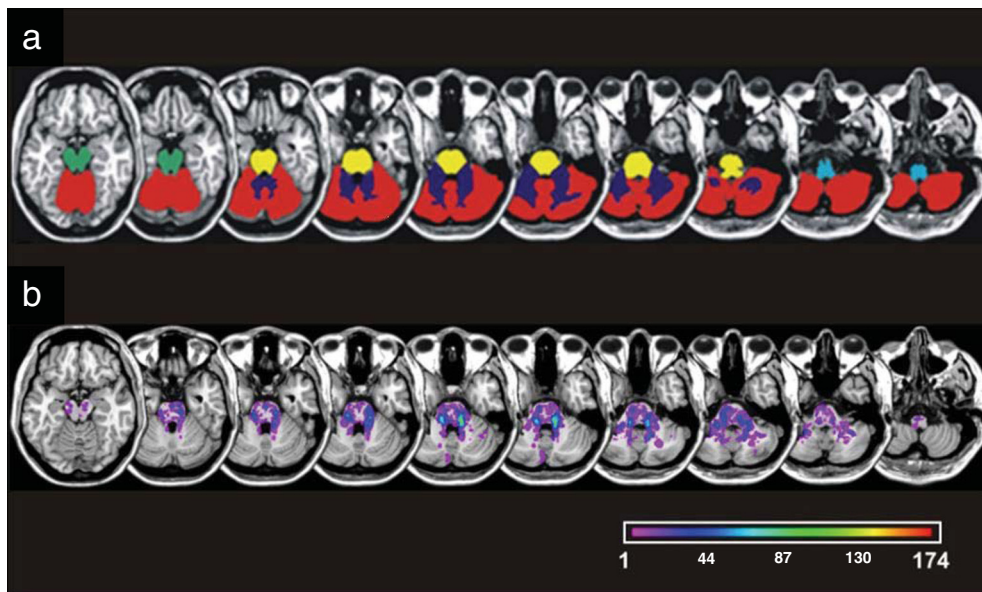


Fig. 1. Lesion overlay map of infratentorial MS lesions. Lesion overlay map for the observed dissemination of infratentorial MS lesions. (a) Defined regions of the observed areas in the brainstem and cerebellum (red: cerebellar cortical and juxtacortical region; dark blue: peduncles; green: mesencephalon; yellow: pons; bright blue: medulla). (b) Lesion overlay map results for 174 RRMS patients with infratentorial lesions out of the total of 317 patients investigated. The number of overlapping lesions is illustrated by different colors indicating increasing frequencies from violet ($n = 1$) to red ($n = 174$).

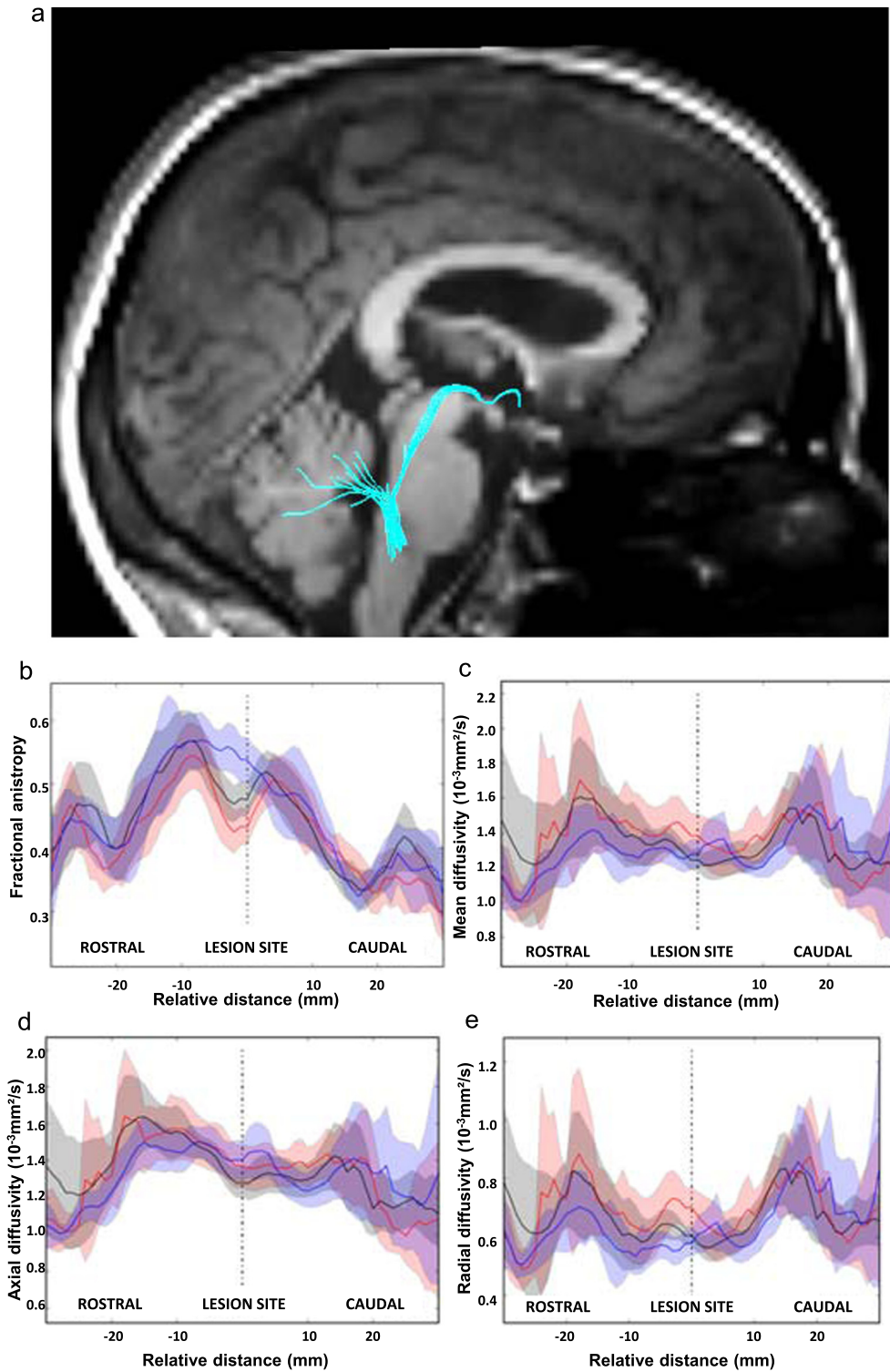


Fig. 3. Diffusion indices along ICP fibers. Diffusion indices plotted along the inferior cerebellar peduncle (ICP) fibers (red: ipsilesional tracts of patients with lesions; black: contralesional tracts of NAWM fibers in the same patients; blue: tracts of healthy controls (HC)). Solid lines represent mean values and the shaded areas correspond to $\pm 1.96 \times$ standard deviation (95% confidence region). (a) Tracked ICP fibers passing through the MS lesion are illustrated. (b) A significant decrease in fractional anisotropy (FA) is observed along ipsilesional fibers compared to the corresponding fibers in HC ($p < 0.05$; Kolmogorov–Smirnov test). No differences in (c) mean diffusion (MD) and (d) axial diffusivity (AD) were found between the groups. (e) Radial diffusivity (RD) is significantly increased along the ipsilesional fibers in comparison with corresponding fibers in HC ($p < 0.05$; Kolmogorov–Smirnov test). In contrast, RD values were not found to differ between ipsilesional and contralesional NAWM tracts.

4. Discussion

The presence of two or more infratentorial lesions in MS patients has been shown to be related to the risk of long-term disability (Minneboo et al., 2004), and thus, infratentorial lesions could be a useful marker for

early identification of a more severe disease course (Tintore et al., 2010). However, the role of lesion location and topography in RRMS remains unclear. The first step in this study was to identify predilection sites of infratentorial lesions in RRMS patients. Our findings, based on data from 317 patients, indicate that within these regions, the pons and

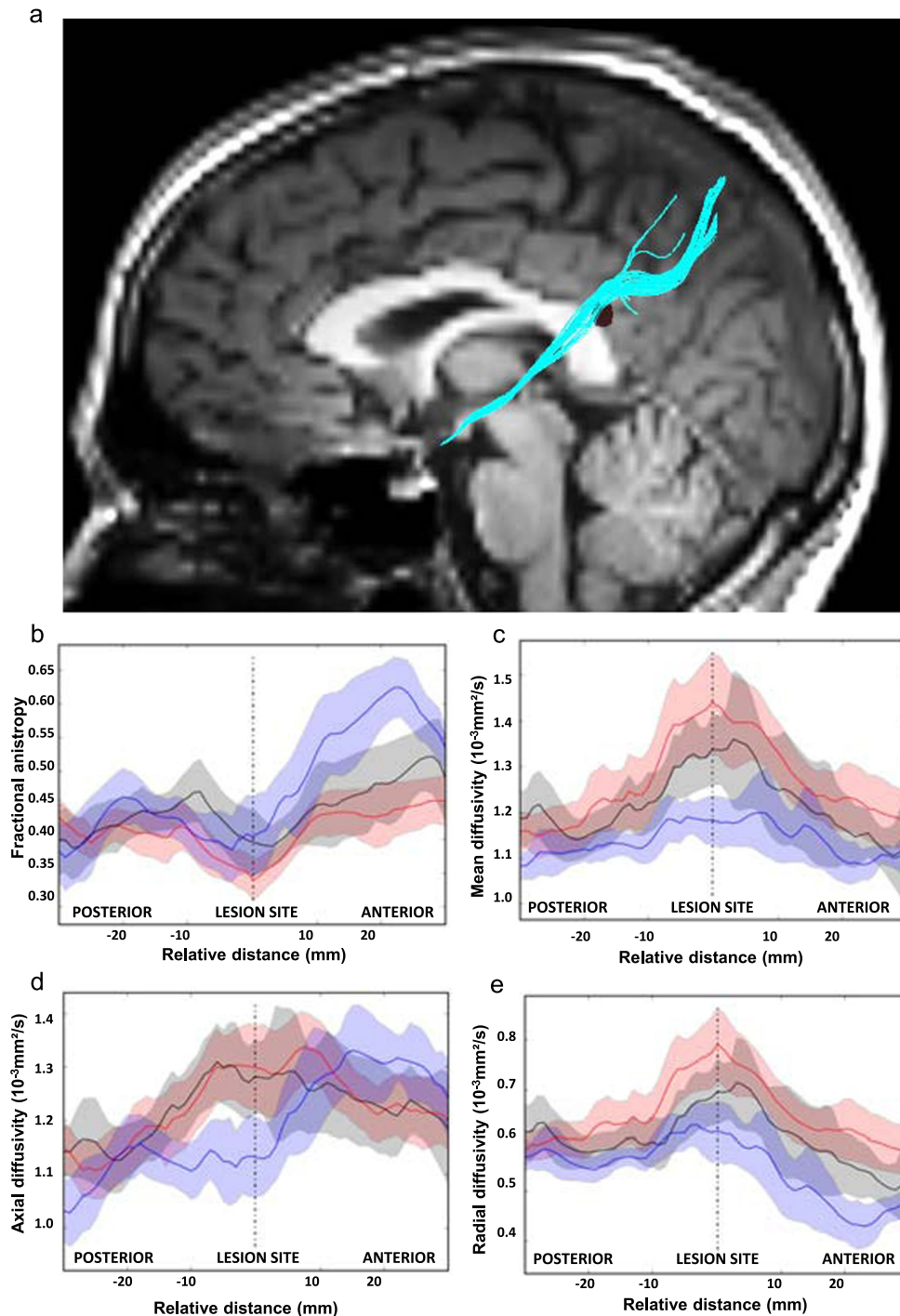


Fig. 4. Diffusion indices along LSAF fibers. Diffusion indices along the left superior arcuate fasciculus (LSAF) fibers (red: fibers of patients with MS lesion; black: contralesional NAWM fibers with no lesions; blue: fibers of healthy controls (HC)). Solid lines represent mean values and the shaded areas correspond to $\pm 1.96 \times$ standard deviation (95% confidence region). (a) Tracked LSAF fibers passing through MS lesion are illustrated. (b) A significant global decrease in fractional anisotropy (FA) values in ipsilesional fibers was found in comparison with contralesional tracts of NAWM in the same patients and HC ($p < 0.01$; Kolmogorov–Smirnov test). (c) A significant increase in mean diffusivity (MD) values was found in the ipsilesional fibers compared with fibers of HC ($p < 0.01$; Kolmogorov–Smirnov test). (d) Axial diffusivity (AD) was found to be decreased in NAWM in comparison with the fibers of HC and ipsilesional fibers. Moreover, significant differences in AD were detected between the tracts of the HC and patients ($p < 0.01$; Kolmogorov–Smirnov test). (e) Radial diffusivity (RD) values were found to be increased in ipsilesional fibers of patients and contralesional NAWM fibers compared to the tracts of the HC group ($p < 0.01$; Kolmogorov–Smirnov test).

cerebellar peduncles were more frequently affected by MS lesions and exhibited markedly increased LD in comparison to the midbrain, cerebellar hemispheres and medulla. Similarly to the periventricular space and corpus callosum, which are the most-reported supratentorial plaque locations (Wahl et al., 2011), the cerebellar peduncles comprise densely packed nerve fibers connecting areas critical for motor, vestibular and ocular motor functions within the CNS (Aboitiz et al., 1992).

These myelinated fibers are parallel laminated in contrast to more diffuse WM fiber pathways. Moreover, the results of our lesion mapping study are consistent with recent data indicating that the pons and cerebellar peduncles are the structures most likely affected by MS lesions in CIS patients with brainstem/cerebellar onset (Giorgio et al., 2013). It should be noted that this preliminary lesion mapping study was performed retrospectively. Future prospective studies should be conducted

to investigate whether there is any correlation between these predilection sites and distinct clinical outcomes.

The main objective of this study was to investigate both the local and distal impact that infratentorial lesions in the areas most affected in MS have on the pathways they interrupt. The present data from 118 investigated fiber bundles (57 ICP and 61 LSAF tracts in 23 RRMS patients and 15 HCs) show distinct alterations in diffusion parameters not only at the lesion site, but along the entire fiber tract. The presence of an MS lesion led to a global reduction in FA and a global increase in RD values along the entire ICP fiber. Our investigation of LSAF fibers affected by a lesion also revealed pathologic diffusivity along the tract, indicating that MS lesions impact WM fibers not only at the lesion site and its immediate surroundings, but rather have extended effects along the entire fiber. These findings are consistent with the hypothesis that increased RD could be a surrogate for demyelination processes (Filippi et al., 2001; Klawiter et al., 2011). Demyelination and axonal pathology have been found not only at lesion sites (Ciccarelli et al., 2008; Filippi et al., 2001; Rovaris et al., 2005) but also in NAWM from post-mortem MS patients (Evangelou et al., 2000); possible mechanistic explanations for why damage extends beyond the lesion vicinity are processes such as Wallerian and retrograde degeneration (Siffrin et al., 2010b). In animal experiments, axonal dysfunction such as long-term calcium upregulation has been found distant from a lesion after attack towards a neurite, suggesting that related destructive processes occur prior to transection; such neuronal dysfunction was found to be potentially reversible (Siffrin et al., 2010a).

In a recent study of cerebellar damage in MS using fiber tractography and volumetric analysis, Anderson et al. (2011) reported decreased FA values of the medial cerebellar peduncles in patients with primary progressive MS compared to those of patients with RRMS and HCs. However, in contrast to our data, no significant differences in FA and RD were reported between RRMS patients and controls. Yet, these data were collected on a 1.5-T scanner and it was not clearly stated whether MS lesions were present along the analyzed fiber tracts. Another study (Wheeler-Kingshott et al., 2012), using a DT template generated from a control population and calculating diffusivity along directions defined in MNI standard space, reported, in contrast to our data, a decrease in AD, but in agreement with our data, an increase in RD in MS patients compared to healthy subjects. It should be noted, however, that these authors used a patient sample in advanced stages of the disease. For epilepsy patients, it has been reported that changes in AD follow a biphasic pattern, increasing shortly after WM injury followed by a decrease after longer time periods (Concha et al., 2006). It is evident that the different patterns of AD observed in the two investigated fiber types likely depend on the “age” of the MS lesion, and thus, early in the disease, changes in diffusion measures, in particular changes in AD, may be blurred (Caramanos et al., 2012; Li et al., 2006) as a result of the interaction between repair and neuroprotective processes following immune attack and lesion evolution. Therefore, decreases in AD may only be readily detectable at later stages of the disease when axonal damage and clinical symptoms are more pronounced. Longitudinal studies could potentially resolve this issue and offer deeper insight into the AD fluctuations along the affected WM tracts. Nevertheless, the results reported here strongly support the growing evidence that an increase in RD is indeed a sensitive marker for demyelination throughout the disease course (Ciccarelli et al., 2008; Filippi et al., 2001; Klawiter et al., 2011; Rovaris et al., 2005).

The novelty of our study is the investigation of the impact of an isolated MS lesion on WM fibers using DTI and tractography. The changes in diffusivity measures observed in our data suggest alterations along entire fiber tracts as the result of an isolated MS lesion and are an indication of Wallerian degeneration processes even extending to functionally connected brain regions, thus eventually leading to rarefaction and complete destruction or transection of WM fibers from their cell bodies, reducing GM cell densities and/or cortical thickness (Beirowski et al., 2005; Kolasinski et al., 2012). The spatial resolution of the DTI in vivo may not be as high as in animal model experiments using two-photon

microscopy and live imaging (Siffrin et al., 2010a), but our results reveal injured areas at distances exceeding 10 mm beyond the lesion site along the WM tracts. This is in line with previous studies that have reported axonal pathology distal to the site of lesions in vivo in humans with spinal cord injuries (Cohen-Adad et al., 2011a; Schwartz et al., 2005) and DTI changes along WM tracts in post-mortem secondary progressive MS brains (Kolasinski et al., 2012), as well as in animal models of MS and spinal cord injury (Budde et al., 2007; Budde et al., 2008; Cohen-Adad et al., 2008; Cohen-Adad et al., 2011b; DeBoy et al., 2007). Our study demonstrates that changes in diffusivity measures resulting from an isolated lesion are found along the whole affected fiber even at early stages of the disease and emphasizes that increases in RD serve as a strong indication of demyelination processes (Klawiter et al., 2011).

Our unbiased evaluation of lesion accumulation showed that the most affected WM regions within the posterior fossa are the pons and cerebellar peduncles. The latter, whose pathways comprise compact myelinated and parallel-laminated fibers, are comparable to the supratentorial corpus callosum and the periventricular pathways, which are also preferential loci for an immune attack. These findings demonstrate that the immune attack in MS influences more distant networks than expected as the result of a focal inflammatory MS plaque, supporting existing evidence that Wallerian degeneration is an important aspect of the disease pathology. Furthermore, this loss of fiber integrity can be detected in vivo in MS patients using diffusion-weighted imaging techniques.

Acknowledgements

None of the authors report any conflicts of interest relevant to this work. This work was supported by grants from the German Research Council (DFG; CRC-TR 128, B5 to FZ and BA 4097/1-1 to BB) and the Ministry of Science and Education (BMBF/KKNMS, B7.3 to FZ). We wish to thank Christie Dietz and Dr. Darragh O'Neill for proofreading the manuscript.

References

- Aboitiz, F., et al., 1992. Fiber composition of the human corpus callosum. *Brain Res.* 598 (1–2), 143–153. [http://dx.doi.org/10.1016/0006-8993\(92\)90178-C1486477](http://dx.doi.org/10.1016/0006-8993(92)90178-C1486477).
- Anderson, V.M., et al., 2011. A comprehensive assessment of cerebellar damage in multiple sclerosis using diffusion tractography and volumetric analysis. *Mult. Scler.* 17 (9), 1079–1087. <http://dx.doi.org/10.1177/135245851140352821511688>.
- Baier, B., et al., 2012. A pathway in the brainstem for roll-tilt of the subjective visual vertical: evidence from a lesion-behavior mapping study. *J. Neurosci.* 32 (43), 14854–14858. <http://dx.doi.org/10.1523/JNEUROSCI.0770-12.201223100408>.
- Bammer, R., et al., 2000. Magnetic resonance diffusion tensor imaging for characterizing diffuse and focal white matter abnormalities in multiple sclerosis. *Magn. Reson. Med.* 44 (4), 583–591. [http://dx.doi.org/10.1002/1522-2594\(200010\)44:4<583::AID-MRM12>3.0.CO;2-O11025514](http://dx.doi.org/10.1002/1522-2594(200010)44:4<583::AID-MRM12>3.0.CO;2-O11025514).
- Beaulieu, C., 2002. The basis of anisotropic water diffusion in the nervous system – a technical review. *N.M.R. Biomed.* 15 (7–8), 435–455. <http://dx.doi.org/10.1002/nbm.78212489094>.
- Beirowski, B., et al., 2005. The progressive nature of Wallerian degeneration in wild-type and slow Wallerian degeneration (Wlds) nerves. *B.M.C. Neurosci.* 6, 6. <http://dx.doi.org/10.1186/1471-2202-6-615686598>.
- Budde, M.D., et al., 2007. Toward accurate diagnosis of white matter pathology using diffusion tensor imaging. *Magn. Reson. Med.* 57 (4), 688–695. <http://dx.doi.org/10.1002/mrm.2120017390365>.
- Budde, M.D., et al., 2008. Axonal injury detected by in vivo diffusion tensor imaging correlates with neurological disability in a mouse model of multiple sclerosis. *N.M.R. Biomed.* 21 (6), 589–597. <http://dx.doi.org/10.1002/nbm.122918041806>.
- Caramanos, Z., et al., 2012. Large, nonplateauing relationship between clinical disability and cerebral white matter lesion load in patients with multiple sclerosis. *Arch. Neurol.* 69 (1), 89–95. <http://dx.doi.org/10.1001/archneurol.2011.76522232348>.
- Ciccarelli, O., et al., 2008. Diffusion-based tractography in neurological disorders: concepts, applications, and future developments. *Lancet Neurol.* 7 (8), 715–727. [http://dx.doi.org/10.1016/S1474-4422\(08\)70163-718635020](http://dx.doi.org/10.1016/S1474-4422(08)70163-718635020).
- Cohen-Adad, J., et al., 2008. In vivo DTI of the healthy and injured cat spinal cord at high spatial and angular resolution. *Neuroimage* 40 (2), 685–697. <http://dx.doi.org/10.1016/j.neuroimage.2007.11.03118201909>.
- Cohen-Adad, J., et al., 2011a. Demyelination and degeneration in the injured human spinal cord detected with diffusion and magnetization transfer MRI. *Neuroimage* 55 (3), 1024–1033. <http://dx.doi.org/10.1016/j.neuroimage.2010.11.08921232610>.

- Cohen-Adad, J., et al., 2011b. Wallerian degeneration after spinal cord lesions in cats detected with diffusion tensor imaging. *Neuroimage* 57 (3), 1068–1076. <http://dx.doi.org/10.1016/j.neuroimage.2011.04.06821596140>.
- Concha, L., et al., 2006. Diffusion tensor imaging of time-dependent axonal and myelin degradation after corpus callosotomy in epilepsy patients. *Neuroimage* 32 (3), 1090–1099. <http://dx.doi.org/10.1016/j.neuroimage.2006.04.18716765064>.
- Corouge, I., et al., 2006. Fiber tract-oriented statistics for quantitative diffusion tensor MRI analysis. *Med. Image Anal.* 10 (5), 786–798. <http://dx.doi.org/10.1016/j.media.2006.07.00316926104>.
- DeBoy, C.A., et al., 2007. High resolution diffusion tensor imaging of axonal damage in focal inflammatory and demyelinating lesions in rat spinal cord. *Brain* 130 (8), 2199–2210. <http://dx.doi.org/10.1093/brain/awm12217557778>.
- Evangelou, N., et al., 2000. Quantitative pathological evidence for axonal loss in normal appearing white matter in multiple sclerosis. *Ann. Neurol.* 47 (3), 391–395. <http://dx.doi.org/10.1002/ana.1016264>.
- Filippi, M., et al., 2001. Diffusion tensor magnetic resonance imaging in multiple sclerosis. *Neurology* 56 (3), 304–311. <http://dx.doi.org/10.1212/WNL.56.3.30411171893>.
- Giorgio, A., et al., 2013. Location of brain lesions predicts conversion of clinically isolated syndromes to multiple sclerosis. *Neurology* 80 (3), 234–241. <http://dx.doi.org/10.1212/WNL.0b013e31827debeb23223533>.
- Klawiter, E.C., et al., 2011. Radial diffusivity predicts demyelination in ex vivo multiple sclerosis spinal cords. *Neuroimage* 55 (4), 1454–1460. <http://dx.doi.org/10.1016/j.neuroimage.2011.01.00721238597>.
- Kolasinski, J., et al., 2012. A combined post-mortem magnetic resonance imaging and quantitative histological study of multiple sclerosis pathology. *Brain* 135 (10), 2938–2951. <http://dx.doi.org/10.1093/brain/aws24223065787>.
- Li, D.K., et al., 2006. MRI T2 lesion burden in multiple sclerosis: a plateauing relationship with clinical disability. *Neurology* 66 (9), 1384–1389. <http://dx.doi.org/10.1212/01.wnl.0000210506.00078.5c16682671>.
- Lin, F., et al., 2007. Diffusion tensor tractography-based group mapping of the pyramidal tract in relapsing-remitting multiple sclerosis patients. *AJ.N.R. Am. J. Neuroradiol.* 28 (2), 278–282. <http://dx.doi.org/10.1007/s12276-007-9994-4>.
- Miller, D.H., et al., 1987. MR brain scanning in patients with vasculitis: differentiation from multiple sclerosis. *Neuroradiology* 29 (3), 226–231. <http://dx.doi.org/10.1007/BF004517582886954>.
- Minneboo, A., et al., 2004. Infratentorial lesions predict long-term disability in patients with initial findings suggestive of multiple sclerosis. *Arch. Neurol.* 61 (2), 217–221. <http://dx.doi.org/10.1001/archneur.61.2.21714967769>.
- Mori, S., van Zijl, P.C., 2002. Fiber tracking: principles and strategies — a technical review. *N.M.R. Biomed.* 15 (7–8), 468–480. <http://dx.doi.org/10.1002/nbm.78112489096>.
- Pagani, E., et al., 2005. A method for obtaining tract-specific diffusion tensor MRI measurements in the presence of disease: application to patients with clinically isolated syndromes suggestive of multiple sclerosis. *Neuroimage* 26 (1), 258–265. <http://dx.doi.org/10.1016/j.neuroimage.2005.01.00815862226>.
- Polman, C.H., et al., 2011. Diagnostic criteria for multiple sclerosis: 2010 revisions to the McDonald criteria. *Ann. Neurol.* 69 (2), 292–302. <http://dx.doi.org/10.1002/ana.2236621387374>.
- Rocca, M.A., et al., 2013. Wallerian and trans-synaptic degeneration contribute to optic radiation damage in multiple sclerosis: a diffusion tensor MRI study. *Mult. Scler.* 19 (12), 1610–1617. <http://dx.doi.org/10.1177/135245851348514623572238>.
- Rorden, C., et al., 2007. Improving lesion-symptom mapping. *J. Cogn. Neurosci.* 19 (7), 1081–1088. <http://dx.doi.org/10.1162/jocn.2007.19.7.108117583985>.
- Rossi, F., et al., 2012. Relevance of brain lesion location to cognition in relapsing multiple sclerosis. *PLOS One* 7 (11), e44826. <http://dx.doi.org/10.1371/journal.pone.004482623144775>.
- Rovaris, M., et al., 2005. Diffusion MRI in multiple sclerosis. *Neurology* 65 (10), 1526–1532. <http://dx.doi.org/10.1212/01.wnl.0000184471.83948.e016301477>.
- Schwartz, E.D., et al., 2005. Spinal cord diffusion tensor imaging and fiber tracking can identify white matter tract disruption and glial scar orientation following lateral funiculotomy. *J. Neurotrauma* 22 (12), 1388–1398. <http://dx.doi.org/10.1089/neu.2005.22.138816379577>.
- Siffrin, V., et al., 2010a. In vivo imaging of partially reversible th17 cell-induced neuronal dysfunction in the course of encephalomyelitis. *Immunity* 33 (3), 424–436. <http://dx.doi.org/10.1016/j.immuni.2010.08.01820870176>.
- Siffrin, V., et al., 2010b. Multiple sclerosis — candidate mechanisms underlying CNS atrophy. *Trends Neurosci.* 33 (4), 202–210. <http://dx.doi.org/10.1016/j.tins.2010.01.00220153532>.
- Song, S.K., et al., 2003. Diffusion tensor imaging detects and differentiates axon and myelin degeneration in mouse optic nerve after retinal ischemia. *Neuroimage* 20 (3), 1714–1722. <http://dx.doi.org/10.1016/j.neuroimage.2003.07.00514642481>.
- Song, S.K., et al., 2005. Demyelination increases radial diffusivity in corpus callosum of mouse brain. *Neuroimage* 26 (1), 132–140. <http://dx.doi.org/10.1016/j.neuroimage.2005.01.02815862213>.
- Tintore, M., et al., 2010. Brainstem lesions in clinically isolated syndromes. *Neurology* 75 (21), 1933–1938. <http://dx.doi.org/10.1212/WNL.0b013e3181feb26f21098409>.
- Wahl, M., et al., 2011. Motor callosal disconnection in early relapsing-remitting multiple sclerosis. *Hum. Brain Mapp.* 32 (6), 846–855. <http://dx.doi.org/10.1002/hbm.2107121495114>.
- Wakana, S., et al., 2004. Fiber tract-based atlas of human white matter anatomy. *Radiology* 230 (1), 77–87. <http://dx.doi.org/10.1148/radiol.230102164014645885>.
- Walsh, M., et al., 2011. Object working memory performance depends on microstructure of the frontal-occipital fasciculus. *Brain Connect.* 1 (4), 317–329. <http://dx.doi.org/10.1089/brain.2011.003722432421>.
- Wheeler-Kingshott, C.A., et al., 2012. A new approach to structural integrity assessment based on axial and radial diffusivities. *Funct. Neurol.* 27 (2), 85–90. <http://dx.doi.org/10.1007/s11557-012-0007-4>.